Measurement-Based Frame Error Model for Simulating Outdoor Wi-Fi Networks

Paolo Barsocchi, Gabriele Oligeri, and Francesco Potortì

***Abstract*—We present a measurement-based model of the frame error process on a Wi-Fi channel in rural environments. Measures are obtained in controlled conditions, and careful statistical analysis is performed on the data, providing information which the network simulation literature is lacking. Results indicate that most network simulators use a frame loss model that can miss important transmission impairments even at a short distance, particularly when considering antenna radiation pattern anisotropy and multi-rate switching.**

***Index Terms*—Simulation, FER, two-ray, AWGN, fading.**

I. Introduction: context and objectives

THE issue of simulation credibility in the mobile ad hoc networking (MANET) arena is periodically been rediscussed [1]–[3], given the huge number of papers published in this area. A fundamental issue that is often disregarded is how to model the packet loss process as seen by the application and routing software.

Only few researchers have tackled the expensive task of measuring WLANs [4]. This is what we did and what we present in this paper, as part of a framework that includes the preliminary data analysis performed in [5], a fading model and, finally, a comprehensive Wi-Fi rural area propagation model.

In order to measure the characteristics of the channel independently of the protocol, we set IEEE 802.11 parameters to disable retransmissions, fragmentation and RTS/CTS, and to fix the channel rate; additionally, we send frames in ad hoc mode at precisely controlled time instants. To produce a model independent of the cards' radio and antenna characteristics, we summarise them into a single tunable parameter. As a consequence, our results are useful for a wide range of simulation applications. The whole set of measured data can be downloaded from http://wnet.isti.cnr.it/data/wichmo/navacchio and has made available to the scientific community through the CRAWDAD archive at Dartmouth university (US) [6].

We considered outdoor rural areas for our measurements. One reason is that ad hoc networking in rural areas is a key point for many scenarios related to disaster relief, crisis management, isolated and deserted areas, robot and sensor communications. Such scenarios are considered in several European initiatives, for example the GMES (Global Monitoring for Environment and Security), or the FP7 ICT Work Programme Challenge 2 (Cognitive Systems, Interaction, Robotics).

Manuscript received May 6, 2008; revised August 25, 2008; accepted November 12, 2008. The associate editor coordinating the review of this letter and approving it for publication was B. Liang.

This work was supported by the European Commission under the Interactive Media with Personal Networked Devices NoE (InterMedia, IST-38419) within the 6$^{\text{th}}$ Research Framework Programme.

The authors are with the ISTI Institute of CNR, via Moruzzi 1, I-56124 Pisa, Italy (e-mail: {Paolo.Barsocchi, Gabriele.Oligeri, Potorti}@isti.cnr.it).

Digital Object Identifier 10.1109/TWC.2009.060475

Additionally, the Wi-Fi rural network scenario is the standard playground of most MANET simulations, which assume a flat field without either obstacles or interference; in such scenario, packet loss is the outcome of a three-stage process. The lowest-level stage is the frame error process, that is the statistical description of the occurrences of transmitted IEEE 802.11 frames being received in error and discarded, or not received at all. Next comes the ARQ (automatic repeat request) stage described by the MAC layer, whereby the transmitter considers a frame as lost if it does not receive an ACK and retransmits it up to a configurable number of times, typically set to 7. On top of this, Wi-Fi interfaces implement multi-rate switching, by choosing among the available modulations and codings in order to better exploit the instantaneous channel conditions. Applications running on a Wi-Fi network see the outcome of the three stages.

In this paper, we propose a simple yet effective model for the frame error process, which is based on extensive measurements in a rural area made by using two laptops with standard Wi-Fi interfaces. We performed about 150 measurement runs at three different places, located in wide uncultivated fields partially covered with grass, with an unobstructed line of sight and far from buildings, cell phone antennas and power lines. For each run both laptops, running custom software (http://wnet.isti.cnr.it/software/vbrsr), were set in a fixed position on a small table at 1 m height from the ground; one of the laptops sent 200 000 frames, while the other one recorded the relevant data for each received frame.

As far as we know no results have been published of analogous measurement campaigns in controlled conditions. In fact, measurement campaigns have usually been conducted on complex network arrangements [7], or in simple scenarios where ARQ was always used, hiding the underlying frame error process details [8], [9], or else by aggregating many diverse results that sum up different propagation effects [3], [10].

Few works have adopted a scrupulous technique similar to ours to measure frame error rate (FER). In [4] measurements are done at fixed time intervals with ARQ disabled in an indoor environment at different data rates; however, the relationship between FER and received signal level is not investigated. In [9] the authors rely on measurements of the received signal strength indicator (RSSI) as we do, but to our knowledge no published results are available with precise timings at the frame level. In [11] long-distance links using directional antennas are investigated for different fixed rates, different frame sizes, short frame inter-arrival times and long-duration experiments. The received power level is measured with ARQ turned off, a procedure remarkably similar to ours. FER is consistent with propagation theory, something that we

observed too, though in a quite different environment – rural versus long-distance. The main difference with our procedure is that we did not use the card's monitor mode, in order to reproduce a transmission environment more similar to the one we are interested to simulate; moreover, not all wireless cards implement it.

In [12] received power level versus distance in an open field is given with very low detail and precision, and the height of transmitter and receiver from ground is lacking. The results presented do not contradict ours, but exhibit a level of detail so low that they could be used to support almost any conclusion; indeed, the authors claim that their measurements support a model different from ours.

As a consequence of the lack of precise measurements in the literature, common wisdom suggests that models that base correct reception on distance are not realistic [3]. While this assumption is true in indoor scenarios, we found a clear relationship between distance and frame error probability in a rural area. We study this relationship in three steps.

First, we build a path loss model by exploring the relationship between received power level, transmission rate and height of transmitter and receiver from ground. Second, we study a fading model by analysing the slow fading process that affects the received power level. Third, we find a signal reception model by looking at the relationship between the received power level and the frame error process. We then propose a complete frame error model that should prove useful for simulations of mobile ad hoc rural networks. Because of its simplicity, it could be used as a benchmark scenario when evaluating results obtained in more challenging environments.

We compare our frame error model against those implemented in the commonly used simulators for MANETs. Of these, ns-2 is the most popular [2]. Notwithstanding the number of simulators used and the abundance of MANET studies based on them, simulations rely on frame error models that have not been experimentally tested: we are not aware of any experimental measurement campaign that analyses what a good model is for the frame error process in rural-area wireless networks.

II. Path Loss Model

Previous studies found that path loss characteristics in LOS (line of sight) environments are dominated by interference between the direct path and the ground-reflected path [13]. The two-ray path loss model, in the following referred to as *2RM*, is used for predicting the power level at the receiver in these environments. 2RM is characterised by a *break point* that separates the different properties of propagation in near and far regions relative to the transmitter; before the break point, the mean attenuation is close to the free-space path loss $1/d^2$, while after that point it decreases as $1/d^4$.

The *double regression* model suggested in [14] approximates 2RM by using two slopes of -20 and -40 dB/dec which meet at the break point b. This model, also known as *dual-slope* approximation, is the one used in the *two-ray CMU Monarch* model [15], which is part of ns-2, where the break point is set to $4\pi h_t h_r/\lambda$, h_t being the transmitter antenna height, h_r the receiver antenna height and λ the wavelength of the radio signal.

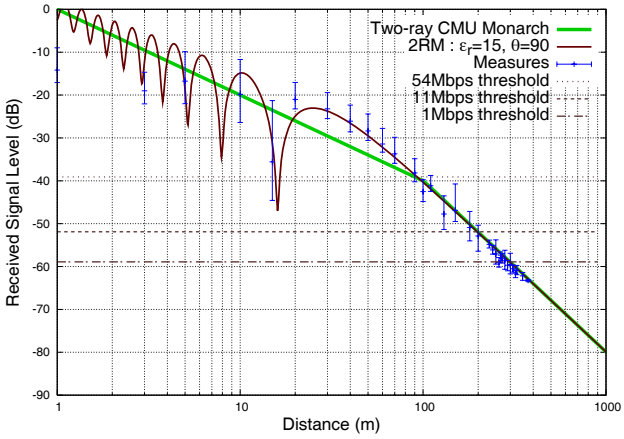

Fig. 1. Measured signal level, two-ray CMU Monarch model and two-ray model with sensitivity thresholds at $\delta_R = 0$ (see Equation (3)). Error bars indicate 0.05, 0.50 and 0.95 quantiles of observed values.

By analysing measurements of RSSI versus distance between transmitter and receiver, it is possible to show that the two-ray path loss model is in fact a better fit for the observed behaviour than its dual-slope approximation for Wi-Fi network simulation in rural areas [5].

As far as popular simulators are concerned, the authors did not find any which implements 2RM: the *two-ray CMU Monarch* path loss model in ns-2 (version 2.32) and the models in Glomosim (version 2.0 and the contemporary Qualnet version) and Opnet (contributed model) all use the dual-slope approximation [16]. Specifically, we suggest that those should be replaced with 2RM. The main reason is that 2RM correctly models the "dip" that we observed in our measurements at a distance of about 15 m. Moreover, the single-slope model used in Omnet++ (using Mobility Framework 2.0p3 [16]) should be replaced by 2RM for simulations of rural areas. The above simulators are used for the majority of simulation studies on MANETs [2].

Figure 1 shows the measured values superimposed on the *two-ray CMU Monarch* model. The 2RM line in Figure 1 is the proposed path loss model, where the signal strength at a distance d is expressed in dB by

$$L_d = 10\log_{10}\left|\frac{1}{d} + \Gamma\frac{e^{j2\pi\frac{\delta_d}{\lambda}}}{d+\delta}\right|^2, \qquad (1)$$

where $\delta_d = \sqrt{(h_t+h_r)^2+d^2} - \sqrt{(h_t-h_r)^2+d^2}$ is the path difference between the direct and the reflected rays, and Γ is the reflection coefficient, which for non-conductive, non-ferromagnetic materials is a real number between -1 and 1, different for parallel (horizontal) and perpendicular (vertical) polarisations:

$$\Gamma_{hor} = \frac{\epsilon_r\sin(\theta) - k}{\epsilon_r\sin(\theta)+k}, \quad \Gamma_{ver} = \frac{\sin(\theta)-k}{\sin(\theta)+k}$$

$$\text{where } k = \sqrt{\epsilon_r - \cos(\theta)^2}, \quad \theta = \arccos\frac{d}{\sqrt{(h_t+h_r)^2+d^2}}.$$

Typical values for the ground relative permittivity ϵ_r are 4, 15, 25, while polarisation of the radio wave may change significantly due to reflection or scattering [17]. Note that the greater the distance d, the less the relevance of ϵ_r; indeed, the

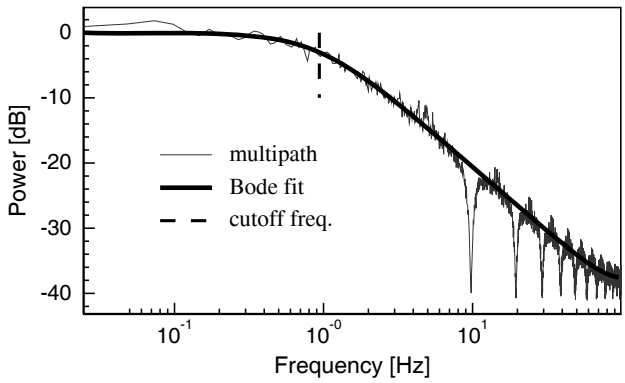

Fig. 2. Power spectrum of the fading process. Pole is at 0.94 Hz.

exact value of ϵ_r is not really important at the distance where the last dip appears and farther away. In practice, the following discussion holds even when the terrain is conductive, for example when it is wet.

In our case, with nodes at 1 m height from the ground, 2RM predicts a dip at 16 m: at this distance the received power, with vertical polarisation and an estimated relative ground permittivity ϵ_r of 15, is the same as the power received at 160 m; the error with respect to the dual-slope model is about 24 dB at that point. This means that, with vertical polarisation, connection can be lost at distances corresponding to the last dip if the transmission range of the card at 11 Mb/s is less than about 160 m. Such transmission range reduction may be consequent to one or more different effects, such as a less sensitive receiver, a channel rate higher than 11 Mb/s, a non-direct antenna orientation, a mismatch between transmitting and receiving antenna polarisation, or scattering due to obstacles close to the transceivers. [5].

This is an important observation, because it means that, with vertical polarisation, connection can be lost at very short distances if the transmission range of the card is less than about 160 m. While, in our measurement, we observed transmission ranges of about 200 m at 11 Mb/s, any reduction in the transmission range will make the effect of the dip apparent and break connectivity. Notice that in real networks connectivity may be preserved thanks to dynamic rate switching, but other effects will occur in a way that is dependent on the dynamic rate switching algorithm: packets will be lost and available bandwidth will shrink, possibly to the point that it becomes insufficient for running applications or that routing algorithms perform badly. These effects are important for simulation studies targeted to either dynamic rate switching algorithms, routing performance or application performance.

III. Slow fading model

We observe that the received signal envelope is modulated by a slow fading process with bandwidth in the range from 0.5 to 1.25 Hz for most of the measurements, with mean and median close to 0.85 Hz. Figure 2 shows how a single-pole spectrum, with aliasing due to sampling, fits the observed power spectrum for a measurement at 230 m distance with 1.66% frame error rate. The dips in the spectrum are at multiples of the reciprocal of 102.4 ms, that is the beacon generation interval. Being an artifact of the MAC access

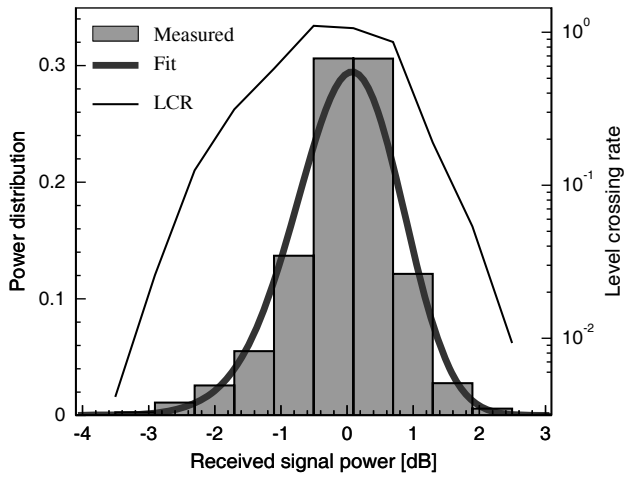

Fig. 3. On the left scale, distribution of received power level and Rician distribution with Rice factor 20.5 dB. On the right scale, level crossing rate. X-axis values are relative to a mean received signal power of 5.6 dB above card sensitivity.

procedure and not a feature of the channel, they have been ignored in the fitting by using appropriate weights.

We attribute fading to multipath effects caused by scattering of the radio waves on terrain features moved by the gentle wind, such as moving grass and possibly moving ground powder; in fact, slow fading due to moving vegetation was also observed in [18]. In order to verify this hypothesis, we look for the signature of multipath fading, by considering the distribution of the received power and its level crossing rate (LCR) statistics.

The fading distribution approximates a lognormal distribution around the mean received power, which is consistent with the Rice distribution to be expected from multipath fading expressed in dB. The Rice factor, that is the ratio of signal power to multipath power, lies in the range from 15 to 25 dB for most of the measurements, with both mean and median close to 19 dB. Both the distribution and the LCR observed on measured data (Figure 3 shows an example for the same measurement as above) are consistent both with what is observed in [18] at slow wind speeds and with the hypothesis of multipath fading.

As far as the dependence of the fading statistics on measurement parameters is concerned, we observe that the power spectrum is remarkably similar for all measurements at distances in the range from 1 m to 300 m, for different channel rates, different packet lengths and channel sampling rates in the range from 50 to 200 frames per second.

The same applies to the Rice factor for distances exceeding 150 m. In the range from few meters to 150 m, the typical bell of the Rice distribution has one to several smaller replicas at lower received power levels. These secondary lobes are at lest 20 times lower (i.e., less frequent) than the main one, and their position is well above the card sensitivity. This can be explained by the receiver occasionally locking on a multipath component which, though attenuated, has sufficient power for correct reception, an explanation which is consistent with the second-order LCR statistics. This is a receiver-dependent effect, so we marked as outliers the samples that are farther from the mode than the maximum value. Without the outliers,

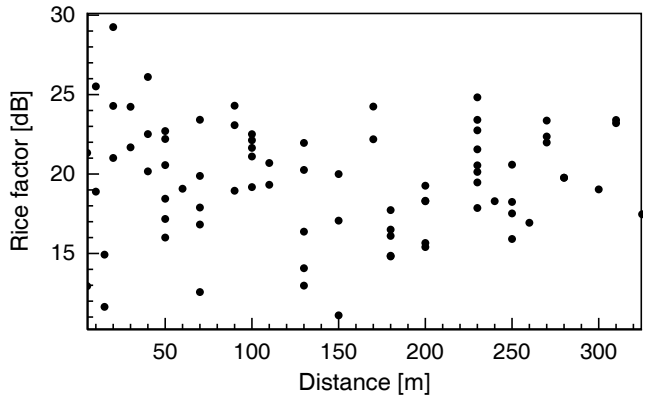

Fig. 4. Rice factor versus distance for measurements with frame error rate smaller than 8% and distance greater than 4 m.

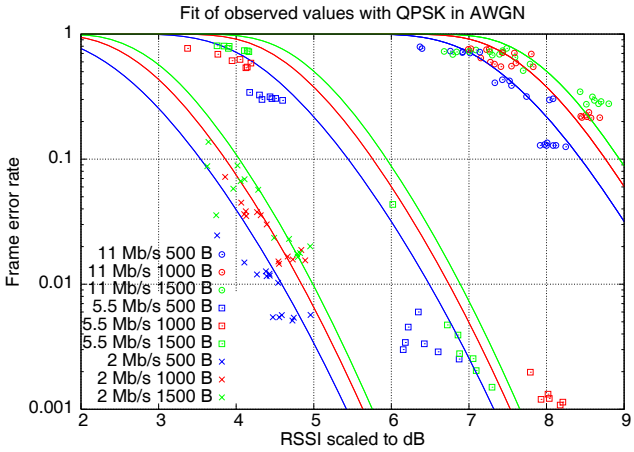

Fig. 5. Fit of Equation (2) with measured values.

the Rice factor statistics are similar for all distances longer than 20 m. At shorter distances, the Rice factor is more widely spread, as shown in Fig. 4; we expected this effect, because cancellation effects in the propagation path produce dips that can strongly amplify small variations of the signal path, as shown in Fig. 1.

The very slow fading we observed is significantly different from the fading models implemented in popular simulators, which ignore correlations between successive frame errors, a problem also observed in [3]. Such fading may have a strong influence on the behaviour of dynamic rate switching algorithms and dynamic routing algorithms that need to evaluate whether two stations are visible each other.

IV. Signal Reception Model

In Section II, we found that 2RM is a good model for predicting the behaviour of RSSI, and in Section III we kept into account the random fading process that affects it. Here we discuss the relationship between RSSI and the frame error process.

The statistical analysis detailed in [5] indicates that for a given RSSI the frame error process is Bernoullian for time scales of few seconds. For longer time spans, the Bernoulli process is modulated by the fading process discussed in Section III.

TABLE I
Rate-dependent parameters in Equation (2).

Bit rate	l_p [byte]	l_d [byte]	g_p [dB]	g_d [dB]
1 Mb/s	6	36 + l_P	+7.9	+7.9
2 Mb/s	6	36 + l_P	+7.9 (+4.9)	+4.9
5.5 Mb/s	6	36 + l_P	+7.9 (+4.9)	+3.0
11 Mb/s	6	36 + l_P	+7.9 (+4.9)	0
6 Mb/s	3	38 + l_P	+5	+5.0
9 Mb/s	3	38 + l_P	+5	+3.5
12 Mb/s	3	38 + l_P	+5	+1.9
18 Mb/s	3	38 + l_P	+5	-0.6
24 Mb/s	3	38 + l_P	+5	-3.8
36 Mb/s	3	38 + l_P	+5	-7.1
48 Mb/s	3	38 + l_P	+5	-11.5
54 Mb/s	3	38 + l_P	+5	-12.8

Modelling the propagation channel as a simple additive white Gaussian noise (AWGN) channel provides a good fit with observed results, as shown in Fig. 5. This contrasts with the simple threshold-based method used in some simulators, such as ns-2, which is deterministic and independent of the length of the frame. The signal reception model for coherent PSK demodulation in AWGN channel with perfect synchronisation relates frame error probability p with header length, data length and received power level:

$$p = 1 - [1 - \mathrm{erp}(R + g_p)]^{8l_p}\,[1 - \mathrm{erp}(R + g_d)]^{8l_d}, \qquad (2)$$

where $\mathrm{erp}(x) = \mathrm{erfc}(10^{\frac{x}{20}})/2$, l_p and l_d are the lengths in bytes of the PLCP header and of the MAC data part, respectively; g_p and g_d are the rate gains in dB for the PLCP header and the payload, respectively, which depend on the transmission rate; R is the ratio of chip energy to noise at the receiver in dB, relative to 11 Mb/s rate.

Header and data lengths are reported in Table I. Rate gains relative to the 11 Mb/s data rate are obtained from [19]–[21]. Header lengths include 8 bytes of LLC+SNAP headers; l_P is the length of payload; g_p for rates of 2, 5.5 and 11 Mb/s are given for both long and (short) preambles.

V. Proposed Frame Error Model

The proposed frame error model is composed of the path loss model, the fading model and the signal reception model described in the previous sections. We give a mathematical description of it together with suggested values for all parameters, simulation criteria and a reference implementation.

Let us define a reference scenario, consistent with our measurements and the receiver sensitivity as defined in IEEE 802.11: consider two stations placed at 1 m height from ground that transmit a sequence of frames with a payload of 1024 bytes at 11 Mb/s, for a FER of 8% at 200 m; from (1), (2) we obtain the relationship in dB $R = L_d + 61.5$.

More generally, the value of R in Equation (2) should be set to

$$R = L_d + 61.5 + \delta_R \qquad (3)$$

where the *path loss offset* δ_R is a value in dB that accounts for transmission power, receiver sensitivity, gain of transmitting and receiving antennas depending on orientation and type, long-term instability of the receiver and possibly near-field scattering due to obstacles near the antennas. The value of the

path loss offset we observed in our experiments varies between -2.3 dB and $+3.4$ dB. We attribute this variability to small changes in the antenna pointing from one measurement to the next or to a slightly different positioning of the laptop on the small table we used, leading to different scattering in the vicinity of antennas.

A Rician fading process with Rice factor equal to 20 dB and coherence time of 1 s should be multiplied by the received power. Accounting for this is especially important for simulations involving still nodes; in fact, for still nodes not using a fading model, the received power is fixed throughout the simulation and dynamic rate switching effects can not be simulated. Let $F(t)$ be the value at time t of the fading process; from (3) the value of R to be used in (2) becomes

$$R = L_d + 61.5 + \delta_R + 20\log_{10}(F(t)). \quad (4)$$

The fading process can be computed as the output of a one-tap autoregressive filter fed by independent samples drawn from a Gaussian distribution with mean 1 and variance 1/100. Alternatively, it can be approximated by a staircase whose value is recomputed once per second from the same distribution.

For a generic simulation we recommend using (2) to compute the FER for each frame, using the parameters listed in Table I and a value for R computed as in (4) and (1). For ϵ_r we recommend a value of 15, and the use of vertical polarisation, which is both commonly used and the worst case. A value of δ_R set to 0 dB means a range of 200 m at 11 Mb/s. If one wants to simulate a receiver with a better/worse sensitivity, the path loss offset δ_R should be increased/decreased. Alternatively, to increase the range by a factor α, δ_R should be set to $40\log_{10}(\alpha)$.

As shown in [3], [5], attenuations up to 10 dB for each of the transmitter and receiver antennas due to mispointing are reasonable assumptions. While this effect is very significant, simulations typically neglect it. In order to account for it, the larger the antenna misalignment is, the smaller the path loss offset between a given pair of nodes should be. For moving nodes, attenuation due to antenna pointing should be modelled as a time-varying path loss offset.

At http://wnet.isti.cnr.it/software/wifiper.m we provide a reference implementation of the described frame error model, written for the free interpreter Octave [22].

VI. Conclusions

We performed a measurement campaign for measuring Wi-Fi RSSI and packet loss in a wide, uncultivated field without obstacles. From the measurement, we obtained a frame error model that is more accurate than models shipped with commonly-used simulators such as ns-2, Glomosim, Opnet and Omnet++, which together account for the majority of published results in the field of wireless simulation at the packet level. We suggest a non-approximated two-ray path loss model coupled with a slow fading model, and a BER signal reception model; we provide details for practical usage of the model together with a reference implementation that additionally caters for ARQ retransmissions. As far as we can tell, this is the first time that experimental data are used to assess a propagation model for simulating MANETs in rural areas.

We expect to observe more realistic protocol behaviour at all layers in MANET simulations when using the proposed model in place of the commonly used ones.

References

[1] T. R. Andel and A. Yasinsac, "On the credibility of MANET simulations," *IEEE Computer*, vol. 39, no. 7, pp. 48-54, July 2006.

[2] S. Kurkowski, T. Tramp, and M. Colagrosso, "MANET simulation studies: The Incredibles," *Mobile Computing Commun. Review*, vol. 9, no. 4, pp. 50-61, 2006. [Online]. Available: http://www.unik.no/personer/adhocnet/2006/articles/Simulation-kurkowski.pdf

[3] D. Kotz, C. Newport, R. S. Gray, J. Liu, Y. Yuan, and C. Elliott, "Experimental evaluation of wireless simulation assumptions," in *Proc. 7th ACM International Symposium Modeling, Analysis Simulation Wireless Mobile Systems (MSWiM '04)*, Venezia, Italy, Oct. 2004, pp. 78-82.

[4] K. Papagiannaki, M. Yarvis, and W. S. Conner, "Experimental characterization of home wireless networks and design implications," in *Proc. IEEE Infocom*, Apr. 2006.

[5] P. Barsocchi, G. Oligeri, and F. Potortì, "Frame error model in rural Wi-Fi networks," in *Proc. International Symposium Modeling Optimization (Wiopt)*, Limassol, Cyprus, Apr. 2007, p. 4146, wiNMee/WiTMeMo workshop.

[6] D. Kotz, T. Henderson, and I. Abyzov, "CRAWDAD data set dartmouth/campus (v. 2004-12-18)," [Online]. Available: http://crawdad.cs.dartmouth.edu/dartmouth/campus, Dec. 2004.

[7] D. Aguayo, J. Bicket, S. Biswas, G. Judd, and R. Morris, "Link-level measurements from an 802.11b mesh network," in *Proc. 2004 Conf. on Applications, Technologies, Architectures*, vol. 34, no. 4, Oct. 2004, pp. 121-132.

[8] G. Anastasi, E. Borgia, M. Conti, and E. Gregori, "Wi-Fi in ad hoc mode: a measurement study," in *Proc. IEEE International Conf. Pervasive Computing Commun. (PerCom)*, Mar. 2004, pp. 145-154.

[9] D. Dhoutaut and I. Guérin-Lassous, "Experiments with 802.11b in ad hoc configurations," in *Proc. 14th IEEE International Symposium on Personal, Indoor and Mobile Radio Commun.*, Beijing, China, Sept. 2003, pp. 1618-1622.

[10] C. Reis, R. Mahajan, M. Rodrig, D. Wetherall, and J. Zahorjan, "Measurement-based models of delivery and interference in static wireless networks," *SIGCOMM Comput. Commun. Rev.*, vol. 36, no. 4, pp. 51-62, 2006.

[11] K. Chebrolu, B. Raman, and S. Sen, "Long-distance 802.11b links: performance measurements and experience," in *Proc. MobiCom*, 2006, pp. 74-85.

[12] M. Zuniga and B. Krishnamachari, "Analyzing the transitional region in low power wireless links," in *Proc. IEEE Sensor Ad Hoc Commun. Networks Conf.*, 2004, pp. 517-526.

[13] A. J. Rustako, N. Amitay, G. J. Owens, and R. S. Roman, "Radio propagation at microwave frequencies for line-of-sight microcellular mobile and personal Commun.," *IEEE Trans. Veh. Techol.*, vol. 40, no. 1, pp. 203-210, Feb. 1991.

[14] E.Green and M. Hata, "Microcellular propagation measurements in a urban environment," in *Proc. PIMRC*, Sept. 1991.

[15] J. Broch, D. A. Maltz, D. B. Johnson, Y.-C. Hu, and J. Jetcheva, "A performance comparison of multi-hop wireless ad hoc network routing protocols," in *Mobile Computing Networking*, 1998, pp. 85-97.

[16] M. Becker, *Personal Communication*. 2007.

[17] T. S. Rappaport, *Wireless Communications*, 2nd ed. Upper Saddle River, NJ (US): Prentice-Hall, 2002.

[18] M. H. Hashim, D. Mavrakis, and S. R. Saunders, "Measurement and analysis of temporal fading due to moving vegetation," in *Proc. International Conf. Antennas Propagation*, vol. 2, Mar. 2003, pp. 650-653.

[19] C. Heegard *et al.*, "High performance wireless Ethernet," *IEEE Commun. Mag.*, vol. 39, no. 11, pp. 64-73, Nov. 2001.

[20] C. Heegard, "Range versus rate in IEEE 802.11g wireless local area networks," presented in September meeting IEEE 802.11 Task Group G, Sept. 2001. [Online]. Available: http://www.nativei.com/~heegard/papers/RvR.pdf

[21] W. Camey, "IEEE 802.11g: new draft standard clarifies future of wireless LAN," Texas Instruments, Tech. Rep., 2002, white paper.

[22] J. W. Eaton and J. B. Rawlings, "Octave–recent developments and plans for the future," in *Proc. 3rd International Workshop Distributed Statistical Computing*, K. Hornik and F. Leisch, eds., Mar. 2003.